# Growth and small-polaron conduction of hole-doped $LaTiO_{3+\delta/2}$ and $NdTiO_{3+\delta/2}$ thin films

J. Li,[1,*] F. B. Wang,[1,2] P. Wang,[1] M. J. Zhang,[1] H. Y. Tian,[1] and D. N. Zheng[1]
[1]*National Laboratory for Superconductivity, Beijing National Laboratory for Condensed Matter Physics and Institute of Physics, Chinese Academy of Sciences, Beijing 100080, China*
[2]*College of Materials Science and Engineering, Sichuan University, Chengdu 610064, China*
(Received 25 January 2006; revised manuscript received 1 November 2006; published 10 May 2007)

$ReTiO_{3+\delta/2}$ (Re=La and Nd) thin films have been deposited on (100)$LaAlO_3$ substrates using the pulsed laser deposition technique. The oxygen content in the formula can be tuned to some extent by carefully adjusting the oxygen pressure during film deposition. When grown at higher oxygen pressures, the films tend to be in their fully oxidized insulating form $Re_2Ti_2O_7$ ($\delta=1, Ti^{4+}$) with a twinned monoclinic structure of $[01\bar{2}]_m$ orientations. When grown in a background vacuum around $5\times10^{-4}$ Pa, the films are lightly hole doped ($\delta\sim0, \sim Ti^{3+}$) and retain the near-cubic perovskite structure with the $[001]_c$ axis perpendicular to the film surface, though high-density defects may exist. These two phases coexist in the films grown at intermediate oxygen pressures. For the vacuum-grown near-cubic films, the antiferromagnetic ordering dies in the lanthanum titanate due to oxygen doping but still survives in the neodymium titanate owing to the higher electron correlation strength in the latter. The transport behavior in the $\sim Ti^{3+}$ Mott insulating films can be described well by the small-polaron hopping or variable range hopping model. In the hole-doped metallic films, a temperature-dependent carrier density and Hall mobility were observed, especially at low temperatures. The temperature dependence of the resistance can be almost perfectly fitted by a small-polaron coherent conduction model $[R_s(T)=R_s(0)+C\omega_\alpha/\sinh^2(T_\omega/T)]$.

DOI: 10.1103/PhysRevB.75.195109 PACS number(s): 72.80.Ga, 73.50.Gr, 81.15.Fg

## I. INTRODUCTION

The titanates $ReTiO_3$ (where Re is a trivalent rare earth) are canonical Mott-Hubbard-type insulators with a $Ti^{3+}$ ($3d^1t_{2g}$) electron configuration and a perovskite structure.[1] It has been widely accepted that the insulating behavior is ascribed to the strong Coulomb repulsion among the integer number of electrons at each Ti site, which opens a charge gap at the Fermi surface. The transport properties are determined by the electron correlation strength $U/W$, where $U$ is the on-site Coulomb energy and $W$ is the one-electron bandwidth. The bandwidth $W$, and hence the correlation strength, can be tuned by varying the $GdFeO_3$-type distortion through changing the average radius of the $A$-site ions or by applying external hydrostatic pressures. A bandwidth-controlled insulator-metal transition can then occur. Alternatively, anomalous metallic states with enhanced electron effective mass can also be derived from the Mott insulators upon hole doping, by substituting the trivalent rare-earth ion with a divalent alkaline-earth ion or by introducing "excess oxygen" ions into the lattice, the so-called filling-controlled insulator-metal transition.

It has been recognized that the fully reduced $Ti^{3+}$ single crystals with a stoichiometric oxygen content of 3.0 can only be acquired in an extremely reducing atmosphere.[2,3] The titanates have a strong tendency to incorporate Re vacancies, which are frequently denoted by excess oxygen in the formula $ReTiO_{3+\delta/2}$.[4] With increase of the nominal hole doping $\delta$, the material evolves from a Mott insulator with a spin and orbital ordering to a paramagnetic heavy metal of filling $1-\delta$. When $\delta$ is larger than a certain value, however, additional oxygen layers appear along the perovskite {110} planes,[5] and the effective carrier density decreases. The end member $ReTiO_{3.5}$ ($Re_2Ti_2O_7$) is a band insulator ($Ti^{4+}, 3d^0$) with a layer-perovskite structure, which becomes ferroelectric at an enormously high transition temperature.[5]

Electronic properties of the doped titanates have been widely studied during the past decade in single crystals. A striking quadratic temperature dependence ($T^2$) of resistivity has been conspicuously observed over a large temperature range in metallic $LaTiO_{3+\delta}$ (Ref. 3) and $Sr_{1-x}La_xTiO_{3+\delta}$,[6] accompanied by a remarkable electron effective-mass enhancement. This had been attributed to the electron-electron correlation in the system. Other characteristic properties, such as temperature-independent Pauli-like susceptibility and the $T$-linear electronic specific heat, were also revealed. The doped titanates were then argued to be described well by the Fermi-liquid picture.

In contrast to the comprehensive investigations on single-crystal bulks, reports on titanate thin films[7–15] are limited in quantity. One possible cause is the huge difficulty in achieving $Ti^{3+}$ compounds. Ohtomo *et al.*[7] have demonstrated that up to six-unit-cell-thick $LaTiO_3$ layers can be stabilized on $SrTiO_3$ at conventional deposition conditions owing to the constrain effect of the substrates. As the film grows thicker, however, a high density of {110} faults (excess oxygen layers) will develop, driven energetically to achieve the equilibrium quadrivalent oxidation state of Ti. Accordingly, most of the $LaTiO_{3+\delta/2}$ films, even prepared in reduced oxygen pressures, behave metallically, although diversity in the absolute resistivity values and the temperature dependencies was noticed. On the other hand, since the bandwidth $W$ in $NdTiO_3$ is narrower than that in $LaTiO_3$ and $U$ in the two systems are equivalent,[16] the Mott insulating state in $NdTiO_{3+\delta/2}$ is much more robust. In this paper, we report our efforts on growing epitaxial thin films of La and Nd titanates on (100)$LaAlO_3$ (LAO) substrates at varied temperatures and oxygen pressures. Mott insulating neodymium titanate thin films with Ti

 

valence of ~3.0 have been successfully obtained. The microstructure and electronic property evolutions with oxygen pressures and temperatures in the as-grown $LaTiO_{3+\delta/2}$ and $NdTiO_{3+\delta/2}$ films are carefully investigated.

## II. EXPERIMENTAL DETAILS

The $LaTiO_{3+\delta/2}$ (LTO) and $NdTiO_{3+\delta/2}$ (NTO) thin films were grown on LAO substrates using the pulsed laser deposition (PLD) technique in a high-vacuum chamber equipped with a high-pressure reflection high-energy electron-diffraction (RHEED) accessory. The ceramic $LaTiO_{3.5}$ and $NdTiO_{3.5}$ targets were fabricated by conventional solid-state reaction at 1370 and 1400 °C, respectively, in air or flowing oxygen for 10 h. The Sr-doped NTO films were prepared by sticking a small piece of $SrTiO_3$ single crystal onto the surface of the ceramic NTO target. A KrF excimer laser with 248 nm wavelength was employed for ablation. The substrate temperatures ($T_S$) were selected between 650 and 850 °C, and the laser energy density was around 2 J/cm$^2$. The films were deposited either in the background vacuum below $5\times10^{-4}$ Pa or at specified oxygen pressures ($P_O$). The deposition lasted for 30 min with a laser repetition rate of 2 Hz. Then, the films were annealed *in situ* for 10 min at the growth $T_S$ and $P_O$ and cooled down in the same ambience to room temperature at a ramp rate of 40 °C/min. The thickness of the films was estimated to be ~2000 Å, using the homoepitaxial growth rate of $SrTiO_3$ in comparable deposition conditions, as determined from the RHEED intensity oscillations.

The crystal structures of these films were monitored *in situ* by RHEED and studied *ex situ* by x-ray diffraction. The electrical resistivity and Hall coefficient were measured using the van der Pauw geometry ($5\times5$ mm$^2$) in the temperature range $5\ \mathrm{K}<T<300$ K. The electrical contacts were made by indium soldering. The magnetic fields for Hall and magnetization measurements were generated by an MPMS-5 (Oxford) superconducting quantum interference device measuring system. Magnetization curves were obtained by first cooling the samples down to 5 K in a 5 T magnetic field and then measuring in a warming-up run in 100 Oe.

## III. EXPERIMENTAL RESULTS

The low-angle sections of the x-ray diffraction (XRD) $\theta$-$2\theta$ diffraction spectra for the titanate thin films deposited at varied conditions are shown in Fig. 1. No impurity phase can be identified in all these spectra. It is noted that the LTO and NTO thin films are roughly similar in that, when grown at high $P_O$, the films show a broad peak at a lower angle around 21.4°, while when grown in vacuum, the peak is sharper and right shifts to a higher angle of ~22.3°. Films deposited at an intermediate $P_O$, say, $1\times10^{-2}$ Pa, possess an even more broad bump just in between (not shown here). The left shift of the diffraction peaks, and thus the change of the out-of-plane $d$ spacing from 3.98 to 4.15 Å with increasing $P_O$, has been previously observed by other research groups.[7,14] Taking the monoclinic bulk data of $LaTiO_{3.5}$ (227 phase) (Ref. 7) and writing them in a habitual way with $a$

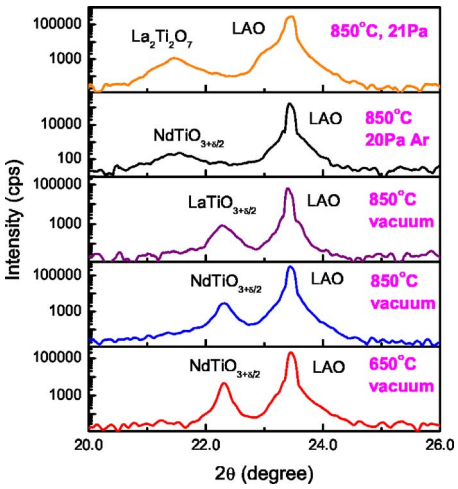


FIG. 1. (Color online) XRD $\theta$-$2\theta$ spectra for the titanate thin films deposited at varied temperatures and ambiences.

$=7.81$ Å $\approx 2a_0$, $b=5.54$ Å $\approx \sqrt{2}a_0$, and $c=13.01$ Å ($a_0$ is the lattice constant of the initial cubic perovskite), one can see that the peaks at lower angles are reflections from the $(01\bar{2})_m$ plane of the 227 phase. Since there are four such equivalent planes due to the twin structures in the 227 films and these planes are not exactly parallel to the film surface but with a small angle (as will be detailed below by RHEED observations), a serious mosaic spread occurs, leading to the very broad and weak peaks in the x-ray spectra. On the other hand, films grown in vacuum retain the perovskite structure, and the peak is from the cubic $(001)_c$ planes. The $d_{(001)c}$-spacing value is slightly longer than the bulk lattice constant of 3.92 Å, most probably due to the biaxial compressive strain from the LAO substrates. Obviously, these two phases coexist in the films grown at intermediate $P_O$. Closely examining the spectra, one can find that the two vacuum-grown NTO films possess peaks narrower than the LTO film grown at comparable conditions, and the peak width for the NTO film deposited at lower $T_S$ is narrower than that at higher $T_S$. The best quality film we ever obtained was the NTO film grown at 650 °C in vacuum, with a full width at half maximum of ~1°. The peak broadening in these cubic perovskite films may have its origin from high-density Re vacancies (and/or {110} faults), i.e., oxygen doping, in the film. Thereby, the data imply that La vacancies are easier to form in LTO films grown at higher $T_S$. This partly explains why Mott insulating $LaTiO_3$ thin films have never been obtained in previous reports. Finally, it is also revealed that Ar ambience helps reserve the oxygen content in the $ReTiO_{3.5}$ targets, so that the film deposited with Ar but in the absence of oxygen also possesses a relatively high oxygen content.

It is known that the oxygen-rich two-dimensional $ReTiO_{3+\delta/2}$ layer perovskite is derived from the cubic lattice by inserting extra oxygen-rich layers along the {110} perovskite planes.[5] Four equivalent such planes exist in the films; accordingly, four types of analogous crystallographic domains with different orientations may exist. Figures 2(a) and 2(b) are the RHEED images for an $LaTiO_{3.5}$ thin film grown

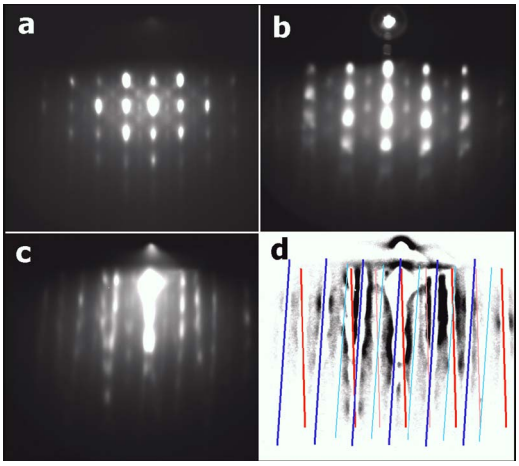


FIG. 2. (Color online) The RHEED images taken along LAO (a) ⟨100⟩ and (b) ⟨110⟩ zone axes, for an $LaTiO_{3.5}$ (227 phase) film grown at 850 °C in $P_O$=22 Pa. (c) An image obtained by turning the incident electron beam slightly away from the ⟨110⟩ direction, and (d) an interpretation of (c), where two sets of tilted streaks with respective angles of 7°–10° are clearly seen.

at 850 °C in 20 Pa oxygen, taken along the LAO ⟨100⟩ and ⟨110⟩ zone axes, respectively. We can see that Fig. 2(a) resembles the Fourier transformation of a high-resolution transmission electron microscopy image of a twinned 227 film.[7] The 45° cross lines in the image are diffractions from the twin boundaries, and the weak spots in between the bright ones reveal a doubled *a*-axis constant due to the monoclinic distortion. The $(01\bar{2})_{227}$ streaks tilt slightly from the surface normal. Diffractions from two types of domains with their $(01\bar{2})$ tilting to opposite directions can be observed along LAO ⟨110⟩, as shown in Fig. 2(b), where the forks at each end of the streaks are obvious. If we then turn the film in plane to deviate the electron beam slightly away from the ⟨110⟩ direction, an image like Fig. 2(c) will appear. As illustrated in Fig. 2(d), the diffractions can be perfectly indexed by two sets of tilted streaks with respective angles within 7°–10°.

The films deposited in background vacuum, however, are three dimensional and epitaxially grown in a cube-on-cube way, with their pseudocubic $(001)_c$ planes parallel to the film surface. As shown in Fig. 3, the RHEED streaks of LTO films [(a) and (b)] are bright and sharp, suggesting good film crystallinity and a smooth film surface. It is noteworthy that the NTO thin films deposited at identical conditions exhibit a superstructure of $2a_0$ in their RHEED patterns [(c) and (d)]. This is due to the stronger $GdFeO_3$-type (orthorhombic) distortion in the latter. In addition, comparing Fig. 3(c), taken after the first 2 min growth at 4 Hz, and Fig. 3(d), taken after the more than 1 h growth, one can conclude that with increase of the film thickness, the film surface becomes more and more rough, as revealed by the three-dimensional diffraction spots in image (d).

In Fig. 4(a), we present the temperature dependencies of resistance for titanate thin films grown at varied substrate temperatures but all in the background vacuum. These films are all pseudocubic. The sample details are listed in Table I.

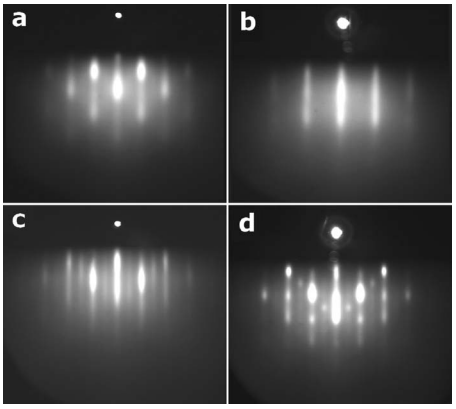


FIG. 3. The (a) ⟨100⟩ and (b) ⟨110⟩ RHEED images for LTO thin films grown at 850 °C in the background vacuum. (e) and (f) are the ⟨100⟩ images of an NTO thin film grown at identical conditions, taken at the initial and final growth stages.

First of all, we note that the LTO film deposited at 650 °C exhibits a typical semiconducting behavior, as also plotted separately in Fig. 4(b). The resistivity at room temperature is about $9.6\times10^{-3}$ Ω cm and the value increases monotonically with decreasing temperature and reaches a fairly high value of $9.3\times10^{-2}$ Ω cm at 5 K. While almost all of the

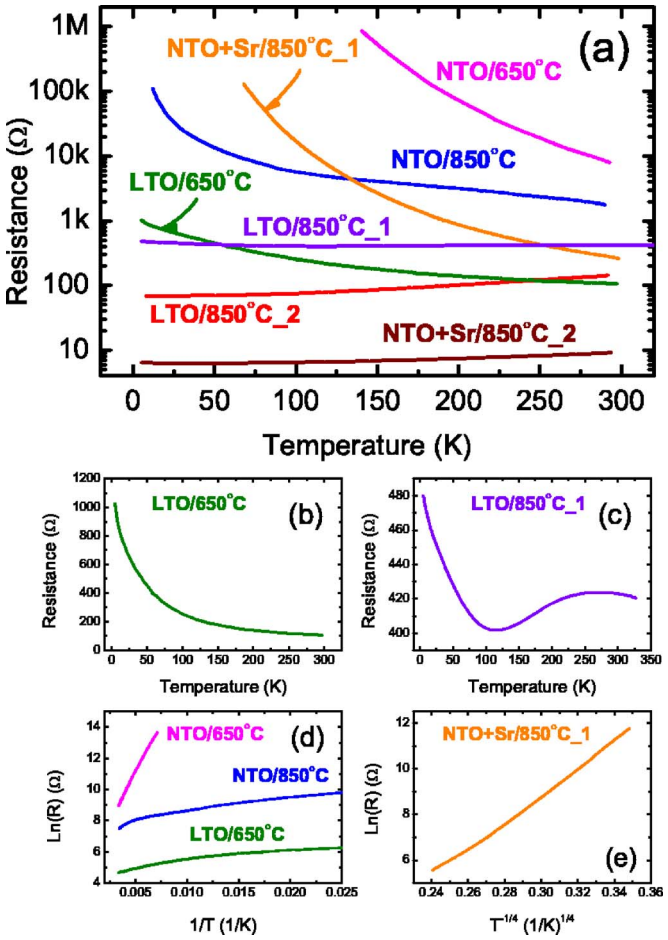


FIG. 4. (Color online) *R-T* curves for the titanate thin films grown on LAO substrates in background vacuum.

TABLE I. Details of the film samples presented in Fig. 4.

| Serial No. | Denotation | Material | $T_S$ (°C) | Vacuum ($10^{-4}$ Pa) | Sr doping (%) | Electrical behavior |
|---|---|---|---|---|---|---|
| 310805 | NTO/650 °C | Nd-Ti-O | 650 | 3.3 | | Insulating |
| 300805 | NTO/850 °C | Nd-Ti-O | 850 | 4.9 | | Insulating |
| 130905 | LTO/650 °C | La-Ti-O | 650 | 3.0 | | Insulating |
| 120505 | LTO/850 °C-1 | La-Ti-O | 850 | 3.1 | | M-I transition |
| 230505 | LTO/850 °C-2 | La-Ti-O | 850 | 5.0 | | Metallic |
| 111005 | NTO+Sr/850 °C-1 | Nd-Ti-O | 850 | 4.6 | 11 | Insulating |
| 241005 | NTO+Sr/850 °C-2 | Nd-Ti-O | 850 | 5.3 | 49 | Metallic |

previously reported pseudocubic La-Ti-O thin films are metallic, we successfully prepared Mott insulating LTO thin films. As is well known, $LaTiO_3$ has been proven to be a Mott insulator located at the immediate vicinity of the metal-insulator boundary, with a moderate electron-electron correlation and a small band gap of 0.2 eV. A slight oxygen excess of ~0.03 would induce metallic behavior,[17] and the three-dimensional metal region in $LaTiO_{3+\delta/2}$ phase diagram spans until $\delta > 0.4$.[5] Thereby, the metal state observed in vacuum-grown LTO films can be easily understood, which remains as long as a moderate $P_O$ is employed. In order to grow in vacuum Mott insulating LTO thin films with trivalent Ti, two factors may be crucial: one is the selection of LAO substrates, as will be further discussed later, and the other one is the substrate temperature control. When grown at a higher $T_S$ of 850 °C, the LTO film shows an S-shaped *R-T* curve, as shown in Fig. 4(c). The resistivity first increases slowly with decreasing temperature, shows a maximum at 270 K, and then decreases again until 110 K, where a drastic upturn occurs. In the view of a large scale, however, as in Fig. 4(a), the resistivity of this sample just changes in a very narrow scope during the whole temperature range measured. Another LTO film deposited also at 850 °C, but perhaps in a poorer vacuum (with more excess oxygen), behaves like a metal, with a slightly lower resistivity. It is apparent that only a small variety of the deposition condition will result in films with distinct transport properties. Since it is difficult to determine the exact oxygen content in films, it is hard to conclude from the data at which oxygen doping level the metal-insulator transition happens.

The two NTO thin films grown in vacuum are all semiconductors and possess an even higher resistivity, obviously due to the larger electron correlation strength. Among the two, the film grown at 650 °C is more "insulating," implying a lower density of Nd vacancies or equivalently a lower density of $Ti^{4+}$ ions in the film, consistent with the XRD results. Using the simple thermal activation model, the energy level in the 650 °C grown NTO film is estimated to be 0.11 eV [shown in Fig. 4(d)], still smaller than the charge gap of pure $NdTiO_3$ single crystal (0.16 eV).[18] This suggests that the Ti valence is still higher than 3.0 even in this most-reduced sample. Figure 4(d) also reveals that the insulating films often deviate from this simple thermal activation model at temperatures below 100 K. Actually, the curves can be fitted better using a small-polaron variable range hopping (VRH) model, as shown in Fig. 4(e) (although for different samples, the exponent factor is not necessarily 1/4), which provides additional evidences that a high density of defects exists in these films. In addition, divalent $Sr^{2+}$ doping brings extra holes into the films, and thus decreases the sample resistivity and even makes it metallic. In Fig. 4(a), we also plot curves for two NTO films with different Sr contents grown in vacuum.

The magnetization versus temperature curves for the LTO and NTO thin films grown at 650 and 850 °C in vacuum are shown in Fig. 5. The samples were measured in a field of 100 Oe applied perpendicular to the film surface. It is clear that the antiferromagnetic (AFM) ordering disappears in the LTO film deposited at 650 °C, even though the film is insulating. The result somewhat disagrees with previous observations, in which the $\delta$ value required to totally suppress AFM ordering (~0.08) is larger than that needed to induce the insulator-metal transition (~0.03).[17] Here, this difference may come from the high-density defects in the films. In contrast, AFM ordering survives in the NTO thin films. The Néel temperature $T_N$ for the two NTO films are all around 60 K in

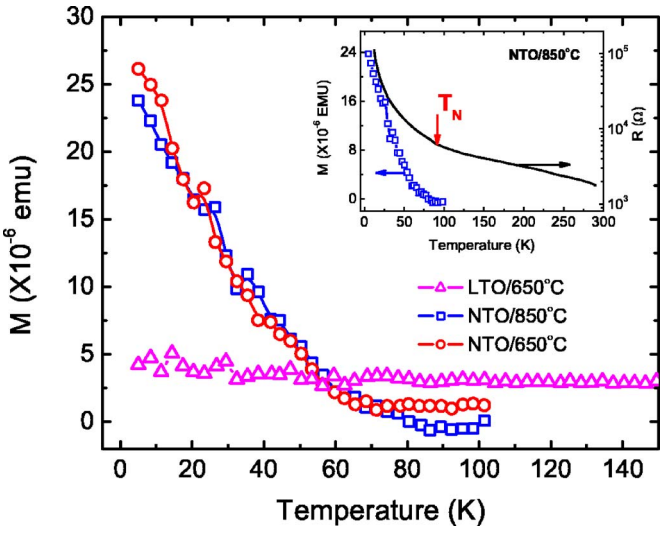


FIG. 5. (Color online) Magnetization curves for vacuum-grown LTO and NTO thin films, measured in a perpendicular magnetic field of 100 Oe [5 T field cooled (Ref. 16)]. Inset shows the correlation between the magnetic ordering and the transport property in the NTO film grown at 850 °C.

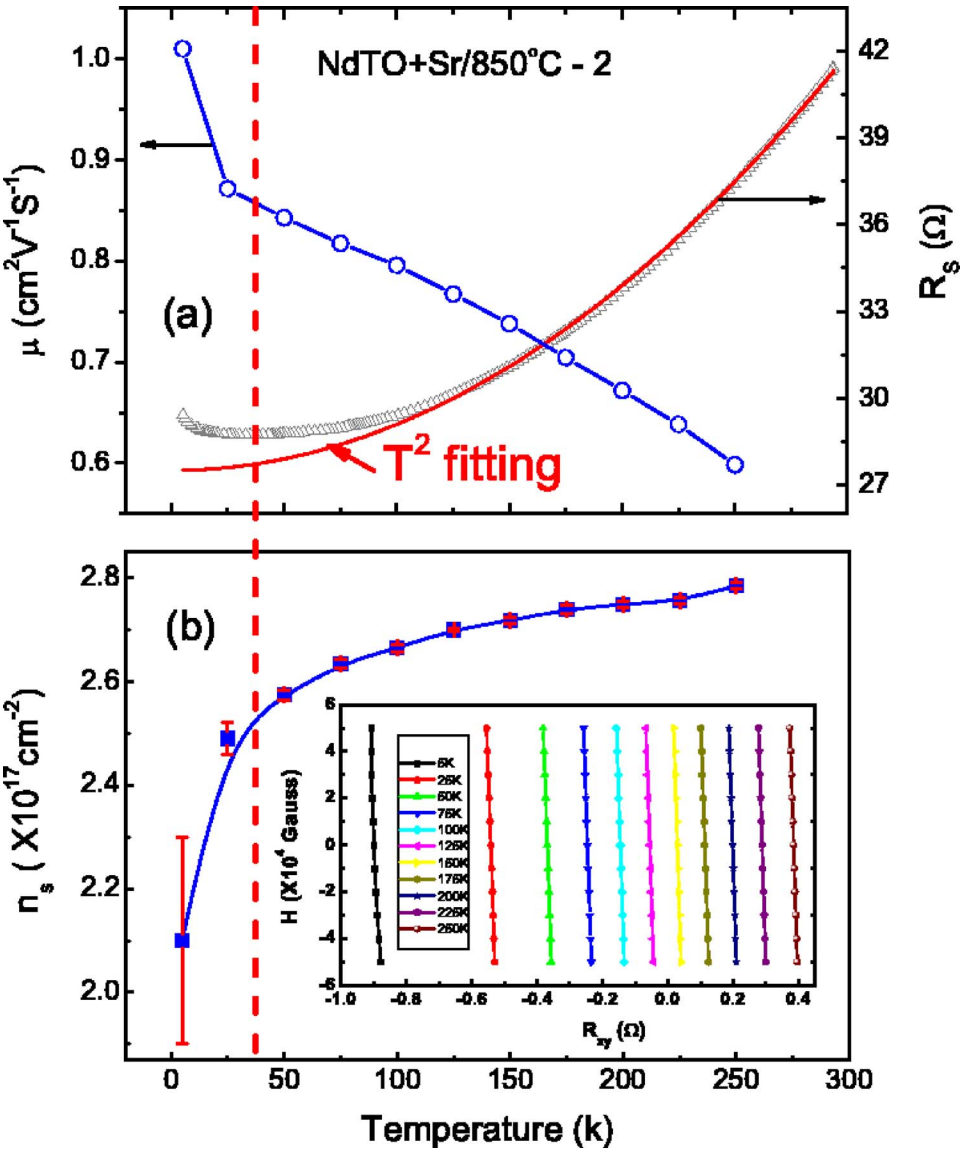


FIG. 6. (Color online) The temperature dependence of $R_s$, $n_s$, and $\mu_H$ for a Sr-doped NTO thin film grown at 850 °C in vacuum. The dash line denotes the M-I transition temperature.

spite of their difference in resistivity, noting that $T_N$ for the undoped $Ti^{3+}$ single-crystal bulk is 90 K.[19] With similar doping, i.e., deposited at identical conditions, AFM ordering is certainly more robust in the much more correlated NTO system. The AFM ordering observed is a solid evidence that the two vacuum-grown NTO films are in the Mott-insulator region with very small hole dopings. The magnetic ordering also has an influence on their transport properties, so that the activation energy changes at $T_N$, as revealed in the inset by the temperature dependence of resistance.

Hereafter, we will focus only on metallic thin films. In Fig. 6(a), we show the temperature dependence of *sheet* resistance for a Sr-doped NTO thin film grown at 850 °C in vacuum. Inductively coupled plasma atomic emission spectrometry reveals that the Nd:Sr ratio in this sample is 1:0.93. This sample behaves metallically at high temperatures but undergoes a clear metal-insulator (M-I) transition at ~20 K. It is noted that the resistivity is roughly $T^2$ dependent but deviates visibly from this law below 120 K. The $T^2$ dependence of resistivity ($\rho=\rho_0+AT^2$) has long been observed in transition metals[20] and later in doped $V_2O_3$ (Ref. 21) and titanate single crystals.[3] It has been attributed to the electron-electron correlation in these systems. The coefficient $A$ in transition-metal iron, nickel, and cobalt are on the order of $1\times10^{-11}$ Ω cm $K^{-2}$, and that in the doped $V_2O_3$ is $5\times10^{-8}$ Ω cm $K^{-2}$. The values in our experiment are determined to be $\sim1\times10^{-8}$ Ω cm $K^{-2}$, comparable to that in $V_2O_3$. Nevertheless, in the electron correlation frame, the $T^2$ dependence is usually dominant only at very low temperatures. A phonon-scattering term shows up as temperature increases. Apparently, our data disagree with this rule. The sample resistance deviates visibly from this law and goes up at a certain temperature, no matter if there is an upturn or not in the $R$-$T$ curves.

Moreover, as shown in Fig. 6(b), Hall measurement demonstrates a clear temperature variation of the effective carrier density in the film,[15] which is again inconsistent with the Fermi-liquid picture. Here, the Hall signal was measured in a perpendicular magnetic field scanned from −5 to +5 T at fixed temperatures. The field ($B$) dependence of the transverse resistance ($R_{xy}$) was recorded. Because of the poor alignment of the voltage electrodes, the transverse voltage

measured in the absence of a magnetic field is nonzero. Anyway, these curves are clearly linear with field, as given in the inset of the figure. The negative slope suggests electron-type carriers. The sheet carrier density $n_s$ can then be precisely read from the slopes of these curves, according to the relationship $n_s=B/eR_{xy}$. The Hall mobility $\mu_H$ was derived using the standard free-carrier formula $\mu_H=1/(qn_sR_s)$, where the $R_s$ value has been obtained in another four-probe measurement system by $R_s=(\pi/\ln 2)R$. The error bar in the figure was added according to the linear fitting errors, which are underestimated because the temperature fluctuations and the geometric irregularity of the electrodes are not considered. As clearly seen, although the sample is a good metal, the derived carrier density declines with decreasing temperature and drops steeply near the M-I transition point. Accordingly, the mobility [shown in Fig. 6(a)] increases gradually with decreasing temperature and rises abruptly around the transition point. In addition, the filling level $1-x-\delta$ in this film should be no more than 0.5 if $\delta>0$, so that the ideal three-dimensional carrier density $n$ should be no more than $8.5\times10^{21}$ cm$^{-3}$. However, the measured $n$ in the sample is higher, being $(1.0-1.4)\times10^{22}$ cm$^{-3}$. Therefore, the Sr-doped NTO film deposited in vacuum may contain oxygen vacancies ($\delta<0$).[22]

## IV. DISCUSSIONS

Most of the literature claimed temperature-independent carrier density, though dissimilarities have also been recorded in lightly doped LTO single crystals (e.g., Fig. 4 in Ref. 17). The carrier density drop and the Hall mobility enhancement at low temperatures have also been observed previously in titanate thin films[22] and explained in terms of the surface band-bending effect.[23,24] Due to the temperature evolution of the film dielectric constant, the thickness of the surface depletion layer grows with cooling, gradually pushing the conduction electrons into the substrate where scattering is reduced. Thus the low-temperature mobility is enhanced. That is, the intrinsic carrier density in the films is temperature independent, but the temperature dependence of the depletion layer reduces the effective carrier number at low temperatures.[22] However, the thickness of our film is around 2000 Å, much thicker than the estimated depletion layer, ~150 Å at 5 K,[22] so it is hard to believe that the temperature dependence of this thin depletion layer can almost double the mobility, as in Fig. 6(a). Relating to their resistivity that does not obey the $T^2$ law, one may conclude that the conduction mechanism in epitaxial titanate thin films may somewhat differ from that in single crystals.

According to Holstein,[25] two different types of small-polaron motion are prevalent at temperatures above or below a certain transition temperature $T_t$. $T_t$ is of the order of $\frac{1}{2}\Theta$ ($\Theta$, Debye temperature) but sensitive to the system parameters. In high temperatures $T>T_t$, the polaron motion predominates by means of a succession of mutually incoherent thermal-activated jumps between neighboring sites, each of which is accompanied by multiple-phonon emission and absorption. With decreasing temperature, the multiphonon process is gradually frozen, and the process involves only a single polaron. As the temperature drops below $\frac{1}{2}\Theta$, the motion is described by hopping due to disorders, and the activation energy is provided by acoustic phonons. When the disorder effect is negligible, in the low-temperature regime $T<T_t$, the hopping activation energy tends to be zero, and the polaron behaves like a heavy particle moving coherently by the usual band mechanism. The width of the "polaron band" exponentially decays with increasing temperature. The fully activated polarons are scattered by thermal phonons and thus the resistivity increases with increasing temperature, exhibiting a metallicklike behavior.

A model of small-polaron metallic conduction has been developed by Bogomolov *et al.*[26] In this model, the resistivity is given by

$$\rho(T)=\rho_0+(\hbar^2/ne^2a^2t_p)\sum_\alpha \frac{A_\alpha\omega_\alpha}{\sinh^2(\hbar\omega_\alpha/2k_BT)},$$

where $n$ is the carrier density, $a$ the lattice constant, $t_p$ the effective hopping integral of polarons, $\omega_\alpha$ the average frequency of one optical phonon mode, and $A_\alpha$ a constant depending on the electron-phonon coupling strength. Assuming that only the low-lying optical mode with a strong electron-phonon coupling contributes to the resistivity, the expression can be simplified as

$$R_s(T)=R_s(0)+C\omega_\alpha/\sinh^2(T_\omega/T),$$

where $R_s$ is the sheet resistance. Zhao *et al.*[27] argued that the metallic transport behavior in doped perovskite manganite thin films could be explained using this law. They have observed a strong oxygen-isotope effect on the intrinsic resistivity in the ferromagnetic metallic state of manganites,[28] which is a solid evidence of the role of phonons in the metallic conduction process in perovskites.

As is well known, in $ReTiO_{3.0}$, the whole $e_g$ orbital is empty and there is only one $t_{2g}$ electron on the $3d$ band. Since the $t_{2g}$ orbital points between $O^{2-}$ in the octahedron, the overlap between titanium $t_{2g}$ and oxygen $2p$ is very weak, resulting in a very narrow conduction band. Small-polaron then is therefore more likely in this system. Actually, transport in lightly electron-doped $TiO_2$ or $SrTiO_3$ has long been attributed to small-polaron coherent conduction mechanism.[29] Here, it is worth mentioning that, in the high-temperature high-vacuum film deposition conditions, oxygen vacancies can be easily developed in $SrTiO_3$ (STO) single-crystal substrates, so that the substrates become electron doped and conducting. Thermodynamically, it is difficult to obtain $Ti^{3+}$ in the film and simultaneously keep $Ti^{4+}$ in the substrate. This is the main reason that we chose only LAO substrates in the experiments. The LAO substrates remain insulating in all the annealing conditions. In the inset of Fig. 7(b), we plot $R_s$ versus $T$ curve for an STO substrate annealed in vacuum at 850 °C for 3 h. The annealed STO itself also shows a metallic behavior, similar to the $ReTiO_{3+\delta/2}$ thin films. The room-temperature resistivity is about $1.9\times10^{-2}$ Ω cm and the value is reduced to $1.4\times10^{-4}$ Ω cm at 5 K. Recently, a number of groups report that the kinetic bombardment of the adatoms on the substrate during growth can induce far more oxygen vacancies in the substrate and

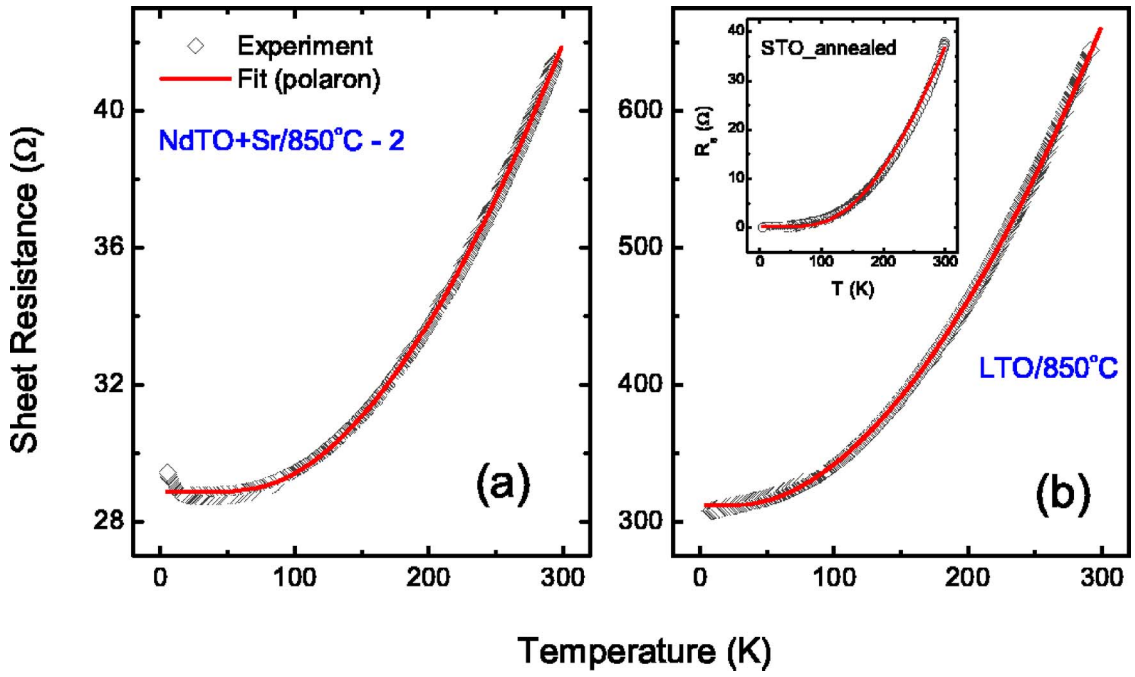


FIG. 7. (Color online) The small-polaron fitting results.

thus further increase its conductivity. We have also noticed that complex phenomena have been observed at the interface of the perovskite oxides and STO substrates, which is a topic of current debate[30–33] but beyond the scope of this study.

We use the above formula to fit the $R_s$-$T$ curves of the annealed STO substrates and the two metallic titanate thin films. The fitting parameters are listed in Table II, and the calculated curves are shown in Figs. 7(a) and 7(b). The fittings were performed without weighting. It is striking that the model can perfectly fit the experimental data for both the STO single crystal and the titanate thin films. Values of the *goodness of fit* $R^2$ for the single crystal is 0.998 and those for the films are even higher, $\geqslant 0.999$. The excellent agreement between the experimental and the calculated curves strongly implies the presence of small polarons and their metallic conduction in the perovskite titanate thin films. The small fitting error may have its origin in that, in the model, the carrier density $n$ is treated as a constant, while, in fact, it changes slowly with temperature. The measured temperature-dependent Hall mobility in our experiments therefore may be attributed to the polaron band width variation with temperature, although we have recognized that the Hall mobility, as affected by higher-order processes of polaron motion, is not equivalent to the drift mobility which is only defined by the lowest order of jump. Gariglio *et al.*[13] also found recently that the small-polaron coherent conduction model could interpret well the transport behavior of their LTO thin films grown on LAO substrates.

By scrutinizing Table II, one can find the following. (a) The residual resistivity is a signature of the crystallinity in the samples. While the annealed single-crystal STO shows the lowest residual resistivity, $\sim 1.55 \times 10^{-4}\ \Omega$ cm, the value is slightly higher for the Sr-doped NTO films, $\sim 5.7 \times 10^{-4}\ \Omega$ cm, and is the largest for the LTO thin film, $\sim 6.2 \times 10^{-3}\ \Omega$ cm. (b) Intuitionally, the constant $C \sim A_\alpha \hbar^2 / n e^2 a^2 t_p$ is roughly proportional to $m^*/n$, where $m^*$ is the effective mass of polarons and $n$ is the carrier density. $C$ manifests its largest value in the vacuum-grown LTO thin film, in which $m^*$ is large due to the small doping level and thus the strong electron-electron correlation in the sample. The heavily doped vacuum-grown NTO thin film exhibits the smallest $C$. Since the film is already away from the Mott-insulator–metal boundary by $Sr^{2+}$ doping, the electron correlation is remarkably weakened so that $m^*$ is small. In the annealed single-crystal STO, $m^*$ is not large and neither is the carrier density $n$, resulting in a moderate $C$ value. (c) The characteristic temperature $T_\omega$ of the phonon coupled to electrons varies from 97 to 270 K in the three samples. This,

TABLE II. Fitting results for the annealed $SrTiO_3$ single-crystal substrate and two other metallic titanate thin films using the small-polaron coherent conduction model.

| Denotation | $R_s(0)$ (Ω) | $C\omega_\alpha$ (Ω) | $C$ ($10^{-14}$ Ω $S^{-1}$) | $T_\omega$ (K) | $\chi^2$ | $R^2$ |
|---|---|---|---|---|---|---|
| STO: annealed | 0.31(3) | 39.1(9) | 55.3 | 270(2) | 0.185 | 0.99796 |
| LTO/850 °C | 312.0(1) | 38.8(9) | 151.7 | 97.90(8) | 1.67078 | 0.99989 |
| NTO+Sr/850 °C-2 | 28.87(4) | 6.34(4) | 12.4 | 194.6(5) | 0.00066 | 0.99996 |

however, disagrees with the argument of Zhao *et al.*[27] that only a dominant optical phonon mode of $\hbar\omega_0/k_B=80$ K contributes substantially to the resistivity in perovskite oxides. This may suggest a flaw of simply attributing the phonon to the tilt and/or rotation of the oxygen octahedra. Other factors, such as the strain from the substrate, may also affect the phonon mode. Further studies are required to clarify this issue.

## V. CONCLUSIONS

In summary, we have deposited LTO, NTO, and NSTO thin films on (100)LAO single-crystal substrates using the PLD technique. The oxygen pressure during film deposition has been carefully controlled so that the filling level $1-\delta$ in the films can be tuned. When grown at high $P_O$, the films are in their fully oxidized insulating form $Re_2Ti_2O_7$ and are monoclinic polycrystalline with domains of different orientations. When deposited in background vacuum or at low $P_O$, the films retain the $ABO_3$ pseudocubic perovskite structure and are epitaxially grown in a cube-on-cube way. The films grown in intermediate $P_O$ are mixtures of the two phases. The films grown in vacuum are mostly Mott insulating and follow a VRH law. The substrate temperature has an influence on the film doping level, with a slightly higher doping at higher $T_S$. The AFM ordering remains in the vacuum-grown NTO thin films but disappears in the vacuum-grown LTO thin films. In addition, the transport behavior of the metallic thin films deviates from the $T^2$ law, and a steep drop of the effective carrier density, and concomitantly a drastic increase of Hall mobility, has been observed at low temperatures. We find that the temperature dependence of resistivity for the metallic films can be described by a small-polaron coherent conduction mechanism.

## ACKNOWLEDGMENTS

The project was sponsored by the National Natural Science Foundation of China under Grants No. 50472076, No. 10574154, and No. 10221002, and the Ministry of Science and Technology, China (2006CB601007). The authors would like to thank H. Yang for his help in the Hall-effect measurements.

*Electronic address: lijie@ssc.iphy.ac.cn

[1] M. Imada, A. Fujimori, and Y. Tokura, Rev. Mod. Phys. **70**, 1039 (1998).
[2] Y. Fujishima, Y. Tokura, T. Arima, and S. Uchida, Phys. Rev. B **46**, 11167 (1992).
[3] Y. Tokura, Y. Taguchi, Y. Okada, Y. Fujishima, T. Arima, K. Kumagai, and Y. Iye, Phys. Rev. Lett. **70**, 2126 (1993).
[4] M. J. MacEachern, H. Dabkowska, J. D. Garrett, G. Amow, Wenhe Gong, Guo Liu, and J. E. Greedan, Chem. Mater. **6**, 2092 (1994).
[5] F. Lichtenberg, A. Herrnberger, K. Wiedenmann, and J. Mannhart, Prog. Solid State Chem. **29**, 1 (2001).
[6] K. Kumagai, T. Suzuki, Y. Taguchi, Y. Okada, Y. Fujishima, and Y. Tokura, Phys. Rev. B **48**, 7636 (1993).
[7] A. Ohtomo, D. A. Muller, J. L. Grazul, and H. Y. Hwang, Appl. Phys. Lett. **80**, 3922 (2002).
[8] A. Ohtomo, D. A. Muller, J. L. Grazul, and H. Y. Hwang, Nature (London) **419**, 378 (2002).
[9] K. Shibuya, T. Ohnishi, M. Kawasaki, H. Koinuma, and M. Lippmaa, Jpn. J. Appl. Phys., Part 2 **43**, L1178 (2004).
[10] A. Schmehl, F. Lichtenberg, H. Bielefeldt, J. Mannharta, and D. G. Schlom, Appl. Phys. Lett. **82**, 3077 (2003).
[11] J. Fompeyrine, J. W. Seo, and J.-P. Locquet, J. Eur. Ceram. Soc. **19**, 1493 (1999).
[12] J. W. Seo, J. Fompeyrine, H. Siegwart, and J.-P. Locquet, Phys. Rev. B **63**, 205401 (2001).
[13] S. Gariglio, J. W. Seo, J. Fompeyrine, J.-P. Locquet, and J.-M. Triscone, Phys. Rev. B **63**, 161103(R) (2001).
[14] K. H. Kim, D. P. Norton, J. D. Budai, M. F. Chisholm, B. C. Sales, D. K. Christen, and C. Cantoni, Phys. Status Solidi A **200**, 346 (2003).
[15] F. B. Wang, J. Li, P. Wang, X. H. Zhu, M. J. Zhang, Z. H. Peng, S. L. Li, L. P. Yong, Y. F. Chen, X. S. Sun, and D. N. Zheng, J. Phys.: Condens. Matter **18**, 5835 (2006).
[16] T. Katsufuji, Y. Taguchi, and Y. Tokura, Phys. Rev. B **56**, 10145 (1997).
[17] Y. Taguchi, T. Okuda, M. Ohashi, C. Murayama, N. Mori, Y. Iye, and Y. Tokura, Phys. Rev. B **59**, 7917 (1999).
[18] K. Yoshii, A. Nakamura, and H. Abe, J. Alloys Compd. **307**, 25 (2000).
[19] G. Amow and J. E. Greedan, J. Solid State Chem. **121**, 443 (1996).
[20] M. Isshiki, Y. Fukudat, and K. Igaki, J. Phys. F: Met. Phys. **14**, 3007 (1984).
[21] D. B. McWhan, A. Menth, J. P. Remeika, W. F. Brinkman, and T. M. Rice, Phys. Rev. B **7**, 1920 (1973).
[22] A. Ohtomo and H. Y. Hwang, Appl. Phys. Lett. **84**, 1716 (2004).
[23] Y. Harumaya, Y. Aiura, H. Bando, H. Suzuki, and Y. Nishihara, Physica B **237-238**, 380 (1997).
[24] Y. Aiura, I. Hase, H. Bando, T. Yasue, T. Saitoh, and D. S. Dessau, Surf. Sci. **515**, 61 (2002).
[25] T. Holstein, Ann. Phys. (N.Y.) **8**, 325 (1959).
[26] V. N. Bogomolov, E. K. Kudinov, and Y. A. Firsov, Sov. Phys. Solid State **9**, 2502 (1968).
[27] G. M. Zhao, V. Smolyaninova, W. Prellier, and H. Keller, Phys. Rev. Lett. **84**, 6086 (2000).
[28] G. M. Zhao, D. J. Kang, W. Prellier, M. Rajeswari, H. Keller, T. Venkatesan, and R. L. Greene, Phys. Rev. B **63**, 060402(R) (2000).
[29] I. G. Austin and N. F. Mott, Adv. Phys. **18**, 41 (1969).
[30] A. Ohtomo and H. Y. Hwang, Nature (London) **427**, 423 (2004).
[31] A. Kalabukhov, R. Gunnarsson, J. Börjesson, E. Olsson, T.

Claeson, and D. Winkler, Phys. Rev. B **75**, 121404(R) (2007).
[32] W. Siemons, G. Koster, H. Yamamoto, W. A. Harrison, T. H. Geballe, D. H. A. Blank, and Ma. R. Beasley, arXiv:cond-mat/0603598 (unpublished).
[33] G. Herranz, M. Basletic, M. Bibes, C. Carretero, E. Tafra, E. Jacquet, K. Bouzehouane, C. Deranlot, J.-L. Maurice, A. Hamzic, J.-P. Contour, A. Barthelemy, and A. Fert, arXiv:cond-mat/0606182 (unpublished).